Journal of Computational Physics 253 (2013) 259–277

Contents lists available at SciVerse ScienceDirect

Journal of Computational Physics

www.elsevier.com/locate/jcp

On particle movers in cylindrical geometry for Particle-In-Cell simulations

G.L. Delzanno *, E. Camporeale

T-5 Applied Mathematics and Plasma Physics Group, Los Alamos National Laboratory, Los Alamos, NM 87545, USA

ARTICLE INFO

Article history:
Received 24 October 2012
Received in revised form 14 May 2013
Accepted 8 July 2013
Available online 15 July 2013

Keywords:
Equation of motion
Particle orbit integration
Boris' mover
Electromagnetic particle simulations
Strang operator splitting
Particle-In-Cell
Second order particle orbit integrator
Cyclotronic mover

ABSTRACT

Three movers for the orbit integration of charged particles in a given electromagnetic field are analyzed and compared in cylindrical geometry. The classic Boris mover, which is of leap-frog type with position and velocities staggered by half time step, is connected to a second order Strang operator splitting integrator. In general the Boris mover is about 20% faster than the Strang splitting mover without sacrificing much in terms of accuracy. Furthermore, the Boris mover is second order accurate only for a very specific choice of the initial half step needed by the algorithm to get started. Unlike the case in Cartesian geometry, where any initial half step which is at least first order accurate does not compromise the second order accuracy of the method, in cylindrical geometry any attempt to use a more accurate initial half step does in fact decrease the accuracy of the scheme to first order. Through the connection with the Strang operator splitting integrator, this counter-intuitive behavior is explained by the fact that the error in the half step velocities of the Boris mover is proportional to the time step of the simulation.

For the case of a uniform and static magnetic field, we discuss the leap-frog cyclotronic mover, cylindrical analogue of the cyclotronic mover of Ref. [L. Patacchini and I. Hutchinson, *J. Comput. Phys.* 228 (7), 2009], where the step involving acceleration due to inertial forces is combined with the acceleration due to the magnetic part of the Lorentz force. The advantage of a cyclotronic mover is that the gyration of a charged particle in a magnetic field is treated analytically and therefore only the dynamics associated with the electric field needs to be resolved.

1. Introduction

Particle-In-Cell (PIC) simulations are unarguably the most popular tool to study the microscopic evolution of a plasma [1,2]. In PIC, a number of computational particles (also called macroparticles or superparticles, each representing a large number of actual particles of the physical system under consideration) move through a computational grid where the field equations are solved. It is the interplay between the grid and the macroparticles that makes PIC an efficient method: the complexity of the algorithm scales linearly with the number of macroparticles (which is much bigger than the number of grid points), as opposed to the quadratic scaling typical of molecular dynamics or N-body methods [2].

From this premise, it is clear that the particle mover is a critical component of any PIC simulation, as it is typically the most time consuming part of the algorithm. As a figure of merit, nowadays explicit electromagnetic PIC simulations with about a trillion particles moved for several ten thousands time steps are becoming doable on modern supercomputers [3]. Therefore it is obvious that fast and accurate methods to simulate the particle orbit are mandatory.

* Corresponding author.
E-mail addresses: delzanno@lanl.gov (G.L. Delzanno), enrico@lanl.gov (E. Camporeale).

0021-9991/$ – see front matter
http://dx.doi.org/10.1016/j.jcp.2013.07.007

Among the various explicit particle orbit integrators that have been proposed to simulate the motion of charged particles in an electromagnetic field, the Boris mover [4] is perhaps the most widely used. As discussed for instance in Ref. [5], one of the reasons for such popularity stems from the fact that the algorithm is relatively easy to implement and retains second order accuracy with only one force evaluation per time step. Other methods such as the second order Runge–Kutta method [6] require two force evaluations per time step. A second reason involves the fact that the Boris mover is time reversible, which means that in certain limits numerical errors on the conservation of certain quantities (for instance energy or angular momentum) are bounded [7]. A third reason is that the algorithm readily extends to the relativistic case.

The focus of this paper is on the analysis of movers in cylindrical geometry, in which inertial forces have to be accounted for in addition to the electromagnetic force. We limit the discussion to movers that are (1) explicit (since the target application is PIC, which typically employs an explicit particle mover), (2) time reversible (since this property is typically associated with error bounds), and (3) second order accurate. The latter is again typical in PIC, and it is a reasonable trade-off between accuracy and speed. We put a strong emphasis on the cylindrical Boris mover, which is applied for instance in Refs. [8–12]. This is a leap-frog type algorithm, where positions and velocities of the particles are staggered in time by $\Delta t/2$ (with Δt the time step of the simulation). Unlike its Cartesian analogue, where at each step of the algorithm only one variable (position or velocity) is updated and the other variable remains fixed, in the cylindrical Boris mover the position update also involves a velocity update. This step corresponds to an exact update of the particle position and velocity under the action of inertial forces only. Furthermore, we show that the cylindrical Boris mover can be connected to a symmetrized, second order Strang operator splitting method [13] which alternates two half steps with acceleration due to the electromagnetic force and one full step with acceleration due to the inertial forces. For the case where a finite magnetic field is present, the Boris mover and the Strang mover are not the same, but they are both second order accurate methods. We have compared both methods on test particle simulations and concluded that the Boris method is about 20% faster without sacrificing much in terms of accuracy. We have also analyzed the choice of the initial half step needed by the Boris algorithm to get started and its influence on the overall accuracy of the scheme. While in Cartesian geometry one can choose any initial half step that is at least first order accurate without compromising the second order accuracy of the method, in cylindrical geometry this is possible for only one choice of the initial step. Therefore, attempts to start the algorithm with a more accurate initial step do decrease the accuracy of the algorithm to first order. This counter-intuitive behavior is due to the fact that in cylindrical geometry the half step velocities of the Boris algorithm have errors proportional to Δt.

For the case of a uniform and static magnetic field, the steps of the Boris method can be rearranged differently by combining the update due to the inertial forces with the update due to the magnetic part of the Lorentz force. This gives rise to the cylindrical leap-frog cyclotronic mover, analogue of the cyclotronic mover presented in Ref. [5] in Cartesian geometry, which is second order accurate, symplectic and time reversible. It treats the gyration motion of a particle in a magnetic field analytically, and therefore one only needs to resolve the dynamics associated with the electric field. The application with a uniform and static magnetic field is relevant to electrostatic PIC simulations of the charging and shielding of objects in a magnetized plasma [14–16]. In this case the cyclotronic mover can be a considerable advantage for strongly magnetized plasmas, since it relaxes the time step constraint imposed by the particle motion perpendicular to the magnetic field [5].

The paper is organized as follows. In Section 2 we describe the Boris algorithm in Cartesian and cylindrical geometry for a charged particle moving in a given electromagnetic field, while in Section 3 we study its accuracy in time, also considering the influence of the initial step needed by the algorithm to get started. In Section 4, we introduce a second order Strang operator splitting method to solve for the particle dynamics and show how this can be connected to the Boris algorithm. This analysis also highlights how the initial half step in the Boris mover needs to be chosen carefully for the method to be second order accurate. In Section 5 we perform some numerical simulations on particle motion in a given electromagnetic field that confirm numerically the theoretical findings. In Section 6, we analyze the case of a uniform and static magnetic field and derive the cylindrical analogue of the cyclotronic mover presented in Ref. [5]. Conclusions are drawn in Section 7.

2. The Boris mover

We study the motion of charged particles in a given electromagnetic field, according to Newton's equations:

$$\frac{d\mathbf{x}}{dt} = \mathbf{v}, \tag{1}$$

$$m\frac{d\mathbf{v}}{dt} = q\big[\mathbf{E}(\mathbf{x}) + \mathbf{v}\times\mathbf{B}(\mathbf{x})\big], \tag{2}$$

where $\mathbf{x}$ ($\mathbf{v}$) is the position (velocity) of the particle with mass m and charge q, while $\mathbf{E}$ ($\mathbf{B}$) is the given electric (magnetic) field.

As we have argued in the introduction, the Boris mover [4] is probably the most widely used algorithm for the numerical integration of Eqs. (1) and (2). We briefly describe the algorithm in this section, focusing on its application to Cartesian geometry, and on its modification in cylindrical geometry.

2.1. Cartesian geometry

In Boris' algorithm, position and velocities of the particles are staggered in time, shifted by $\Delta t/2$. Thus, the Boris mover is a leap-frog type algorithm [1]. Specifically, velocities are at time $t = t^{n+1/2} = (n + \frac{1}{2})\Delta t$ (labeled in the following with superscript $n + 1/2$), while positions are at time $t = t^n = n\Delta t$ (labeled with superscript n).

For the momentum equation update from $n - 1/2$ to $n + 1/2$, the algorithm separates completely the electric and magnetic part of the Lorentz force and consists of the following three steps:

(1) Perform a half step update (time step $\Delta t/2$) with acceleration due to the electric field only:

$$\mathbf{v}^- = \mathbf{v}^{n-1/2} + \frac{q}{m}\mathbf{E}\big(\mathbf{x}^n\big)\frac{\Delta t}{2}. \tag{3}$$

(2) Perform a full step rotation (time step Δt) due to the magnetic field:

$$\mathbf{v}' = \mathbf{v}^- + f^{n,\Delta t}\mathbf{v}^- \times \mathbf{B}\big(\mathbf{x}^n\big), \tag{4}$$

$$\mathbf{v}^+ = \mathbf{v}^- + \frac{2f^{n,\Delta t}}{1 + (f^{n,\Delta t})^2\mathbf{B}(\mathbf{x}^n)^2}\mathbf{v}' \times \mathbf{B}\big(\mathbf{x}^n\big), \tag{5}$$

with

$$f^{n,\Delta t} = \frac{\tan(\frac{q}{m}\frac{\Delta t}{2}|\mathbf{B}(\mathbf{x}^n)|)}{|\mathbf{B}(\mathbf{x}^n)|}. \tag{6}$$

(3) Perform a half step update (time step $\Delta t/2$) with acceleration only due to the electric field:

$$\mathbf{v}^{n+1/2} = \mathbf{v}^+ + \frac{q}{m}\mathbf{E}\big(\mathbf{x}^n\big)\frac{\Delta t}{2}. \tag{7}$$

Once the velocity update is completed, the position can be updated straightforwardly by

$$\mathbf{x}^{n+1} = \mathbf{x}^n + \mathbf{v}^{n+1/2}\Delta t. \tag{8}$$

This algorithm is second order accurate and time reversible [1], but is in general not symplectic. Of course, as for any leap-frog algorithm, the accuracy also depends on the choice of the initial step that needs to be provided to relate the (known) particle position and velocity at time $t = 0$ to the velocity $\mathbf{v}^{-1/2}$ (or $\mathbf{v}^{1/2}$) that the algorithm needs to get started.

2.2. Cylindrical geometry

We now discuss the application of the Boris algorithm to cylindrical geometry. First, we recall the coordinate transformation from Cartesian (x, y, z) to cylindrical (r, θ, z) geometry:

$$\begin{aligned} x &= r\cos\theta, \\ y &= r\sin\theta, \\ z &= z, \end{aligned} \tag{9}$$

and the fact that now the equation of motion of a particle must account for the inertial forces $\mathbf{F}_{in}$ that are associated with such transformation:

$$m\frac{d\mathbf{v}}{dt} = q(\mathbf{E} + \mathbf{v} \times \mathbf{B}) + \mathbf{F}_{in}. \tag{10}$$

In components, we have

$$\frac{dr}{dt} = v_r, \tag{11}$$

$$\frac{d\theta}{dt} = \frac{v_\theta}{r}, \tag{12}$$

$$\frac{dz}{dt} = v_z, \tag{13}$$

$$m\frac{dv_r}{dt} = q(E_r + v_\theta B_z - v_z B_\theta) + m\frac{v_\theta^2}{r}, \tag{14}$$

$$m\frac{dv_\theta}{dt} = q(E_\theta - v_r B_z + v_z B_r) - m\frac{v_r v_\theta}{r}, \tag{15}$$

$$m\frac{dv_z}{dt} = q(E_z + v_r B_\theta - v_\theta B_r), \tag{16}$$

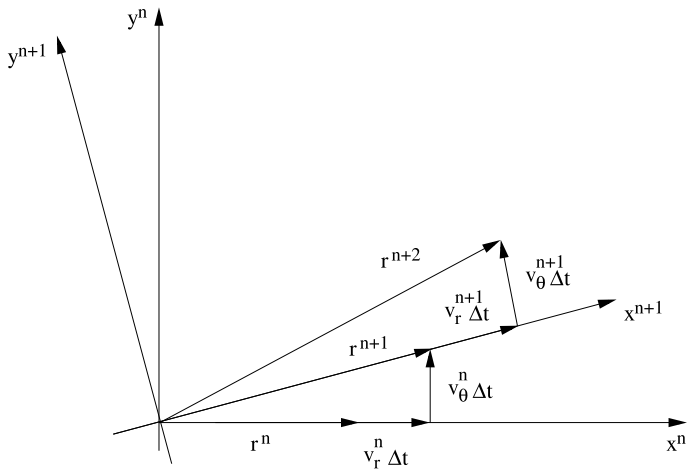

Fig. 1. The change of reference frame of a particle in cylindrical geometry due to its motion: the new velocities are given by Eqs. (21) and (22).

and clearly $\mathbf{F}_{in} = (m\frac{v_\theta^2}{r}, -m\frac{v_r v_\theta}{r}, 0)$. Eqs. (11)–(16) immediately reveal a singularity at $r = 0$ when a particle has finite angular momentum, and the potential for numerical problems there. However, Boris [4] proposed an algorithm that completely bypasses this problem by taking advantage of the Cartesian to cylindrical coordinate transformation. In essence, the momentum equation update remains the same as described in Section 2.1, with the obvious substitution of x, y with r, θ and, most important, *without including inertial forces*. For the position update, the idea is to advance the particle position in Cartesian geometry and then calculate the new r and θ coordinates. More specifically, one defines

$$x^{n+1} = r^n + v_r^{n+1/2*}\Delta t, \tag{17}$$

$$y^{n+1} = v_\theta^{n+1/2*}\Delta t, \tag{18}$$

to obtain the new coordinates

$$r^{n+1} = \sqrt{\left(x^{n+1}\right)^2 + \left(y^{n+1}\right)^2}, \tag{19}$$

$$\theta^{n+1} = \theta^n + \alpha. \tag{20}$$

In Eqs. (17) and (18) we have used the $*$ notation to indicate the velocities at time $n+1/2$ obtained from the momentum update of Section 2.1. Clearly, the particle velocity must now be adjusted to account for the new reference frame pointing to the new particle position. See Fig. 1. This is a simple rotation:

$$v_r^{n+1/2} = \cos\alpha\, v_r^{n+1/2*} + \sin\alpha\, v_\theta^{n+1/2*}, \tag{21}$$

$$v_\theta^{n+1/2} = -\sin\alpha\, v_r^{n+1/2*} + \cos\alpha\, v_\theta^{n+1/2*}, \tag{22}$$

where the angle α in Eqs. (20), (21) and (22) is defined by

$$\sin\alpha = \frac{y^{n+1}}{r^{n+1}}, \tag{23}$$

$$\cos\alpha = \frac{x^{n+1}}{r^{n+1}}. \tag{24}$$

We note that transformations (23) and (24) are well defined only if $r^{n+1} \neq 0$. The case $r^{n+1} = 0$ corresponds to a particle that stops on axis, and one can set $\cos\alpha = 1$ and $\sin\alpha = 0$ to impose that the momentum of that particle is purely radial [4].

An important point to consider is that in Cartesian geometry each step of the algorithm updates one variable (position or velocity) while the other variable (velocity or position) remains fixed. This is not the case in cylindrical geometry, where the position update also involves an update of the velocity.

The Boris mover in cylindrical geometry is time reversible, but in general not symplectic. In the literature, it is reported as second order accurate due to time centering [1,4]. However, this is true only for a particular choice of the initial step that relates $\mathbf{v}^{-1/2}$ to the particle position and velocity at time $t = 0$, unlike the case of Cartesian geometry where any choice of the initial step that is at least first order accurate is sufficient for the overall scheme to maintain second order accuracy. This is proven analytically and numerically in the next sections.

3. Accuracy in time of the Boris mover: comparing Cartesian and cylindrical geometries

For simplicity, we specialize the discussion of this section to the case without magnetic field, $\mathbf{B} = 0$. The case with magnetic field is conceptually similar: it only involves lengthier algebra but the conclusions remain the same. However, in Section 5 we will perform numerical simulations that include a finite magnetic field.

3.1. Cartesian geometry

For the sake of the discussion, it is instructive to recall some basic and well established facts about the case of Cartesian geometry. For simplicity we focus on a one-dimensional example and note that without a magnetic field the Boris mover reduces to the classic leap-frog scheme [1]. The equation for the velocity at time $t^{n+1/2}$ can be written as

$$\frac{v^{n+1/2} - v^{n-1/2}}{\Delta t} = \frac{q}{m} E\left(x^n\right). \tag{25}$$

If one expands the velocities in Eq. (25) around t^n,

$$v^{n\pm 1/2} = v^n \pm \dot{v}^n \frac{\Delta t}{2} + \ddot{v}^n \frac{\Delta t^2}{8} + O\left(\Delta t^3\right), \tag{26}$$

where $\dot{v}^n = \frac{dv}{dt}|_{t=t_n}$, and substitutes Eq. (26) into Eq. (25), the second order accuracy of the scheme is recovered:

$$\dot{v}^n = \frac{q}{m} E\left(x^n\right) + O\left(\Delta t^2\right). \tag{27}$$

In this analysis we have taken advantage of the fact that the velocities are known at $n + 1/2$ times and have analyzed the scheme at n where position is defined. We could have easily expanded the equations at $n + 1/2$, defining $v^n = (v^{n+1/2} + v^{n-1/2})/2$, still recovering second order accuracy. Similarly, the same analysis can be trivially conducted on the position part of the scheme.

Since positions and velocities are staggered in time, a second important point relates to the choice of the first step of the algorithm. At time $t = 0$ position and velocity of the particle are known, x^0 and v^0, and one has to construct for instance $v^{-1/2}$ before the leap-frog algorithm can be applied. Let us then analyze the accuracy of the algorithm at $t = 0$. It is easy to construct the first two updates of the algorithm

$$\begin{aligned}
v^{1/2} &= v^{-1/2} + \frac{q}{m} E\left(x^0\right)\Delta t,\\
x^1 &= x^0 + v^{1/2}\Delta t = x^0 + v^{-1/2}\Delta t + \frac{q}{m} E\left(x^0\right)\Delta t^2,\\
v^{3/2} &= v^{1/2} + \frac{q}{m} E\left(x^1\right)\Delta t = v^{-1/2} + \frac{q}{m}\left[E\left(x^0\right) + E\left(x^1\right)\right]\Delta t,\\
x^2 &= x^1 + v^{3/2}\Delta t = x^0 + 2v^{-1/2}\Delta t + \frac{q}{m}\left[2E\left(x^0\right) + E\left(x^1\right)\right]\Delta t^2.
\end{aligned} \tag{28}$$

Clearly, one can obtain an analytic expression for $v^{n+1/2}$ which stems from the model equations we are trying to solve numerically. That is:

$$\begin{aligned}
v^{n+1/2} &= v^0 + \dot{v}^0\left(n + \frac{1}{2}\right)\Delta t + \ddot{v}^0\left(n + \frac{1}{2}\right)^2 \frac{\Delta t^2}{2} + O\left(\Delta t^3\right)\\
&= v^0 + \frac{q}{m} E\left(x^0\right)\left(n + \frac{1}{2}\right)\Delta t + \frac{q}{m}\frac{dE}{dx}\bigg|_0 v^0\left(n + \frac{1}{2}\right)^2 \frac{\Delta t^2}{2} + O\left(\Delta t^3\right).
\end{aligned} \tag{29}$$

We can compare Eq. (29) to its numerical equivalent obtained by applying the steps of the algorithm. Suppose now that we choose $v^{-1/2} = v^0$ and consider for instance $v^{3/2}$. It follows from Eqs. (28) that

$$v^{3/2} = v^0 + 2\frac{q}{m} E\left(x^0\right)\Delta t + \frac{q}{m}\frac{dE}{dx}\bigg|_0 v^0\Delta t^2 + O\left(\Delta t^3\right), \tag{30}$$

where we have used the expansion

$$E\left(x^1\right) = E\left(x^0\right) + \frac{dE}{dx}\bigg|_0 v^0\Delta t + O\left(\Delta t^2\right), \tag{31}$$

which compared to Eq. (29) indicates that the velocity has an error proportional to Δt. While the update in Eq. (25) remains second order accurate, the overall order of accuracy of the scheme inherits that of the initial half step, namely the scheme is only first order accurate. On the other hand, if we choose

$$v^{-1/2} = v^0 - \frac{q}{m} E(x^0) \frac{\Delta t}{2}, \tag{32}$$

then

$$v^{3/2} = v^0 + \frac{3}{2}\frac{q}{m} E(x^0)\Delta t + \frac{q}{m}\frac{dE}{dx}\bigg|_0 v^0 \Delta t^2 + O(\Delta t^3), \tag{33}$$

which indicates that the error in the velocity is proportional to Δt^2 and so is the overall accuracy of the scheme. Choosing an even higher order approximation for $v^{-1/2}$, for instance

$$v^{-1/2} = v^0 - \frac{q}{m} E(x^0) \frac{\Delta t}{2} + \frac{q}{m}\frac{dE}{dx}\bigg|_0 v^0 \frac{\Delta t^2}{8} \tag{34}$$

or the exact value if we already know the solution of the particle trajectory, does not really help since the update in Eq. (25) is still second order accurate and so is the overall accuracy of the scheme. This analysis reminds us that we should be careful in how we choose the initial half step to get $v^{-1/2}$ and that the leap-frog scheme just described is second order accurate provided that the initial half step is at least first order accurate.

3.2. Cylindrical geometry

Let us now turn our attention to the Boris mover in cylindrical geometry and perform the same analysis of accuracy done above. We limit the discussion to the (r,θ) components since in cylindrical geometry the z component is unchanged. From the momentum equations update, Eqs. (3)–(7), we have

$$v_r^{n+1/2*} = v_r^{n-1/2} + \frac{q}{m} E_r^n \Delta t, \tag{35}$$

$$v_\theta^{n+1/2*} = v_\theta^{n-1/2} + \frac{q}{m} E_\theta^n \Delta t, \tag{36}$$

which can be substituted in Eqs. (17), (18) and (19) to obtain

$$r^{n+1} = r^n + v_r^{n-1/2}\Delta t + \left[\frac{q}{m} E_r^n + \frac{(v_\theta^{n-1/2})^2}{2r^n}\right]\Delta t^2 + O(\Delta t^3). \tag{37}$$

In Eq. (37) we have used the Taylor expansion $\sqrt{1+x} = 1 + x/2 - x^2/8 + \cdots$. From this, we can compute

$$\frac{x^{n+1}}{r^{n+1}} = 1 - \frac{(v_\theta^{n-1/2})^2}{2(r^n)^2}\Delta t^2 + O(\Delta t^3), \tag{38}$$

$$\frac{y^{n+1}}{r^{n+1}} = \frac{v_\theta^{n-1/2}}{r^n}\Delta t + \left[\frac{q}{m}\frac{E_\theta^n}{r^n} - \frac{v_r^{n-1/2} v_\theta^{n-1/2}}{(r^n)^2}\right]\Delta t^2 + O(\Delta t^3), \tag{39}$$

where we have used the Taylor expansion $\frac{1}{1+x} = 1 - x + x^2 + \cdots$. From Eqs. (35), (36), (38) and (39), we can calculate the new velocity at time $n+1/2$ by using Eqs. (21) and (22). It follows that

$$\frac{v_r^{n+1/2} - v_r^{n-1/2}}{\Delta t} = \frac{q}{m} E_r^n + \frac{(v_\theta^{n-1/2})^2}{r^n} + \left[2\frac{q}{m}\frac{E_\theta^n v_\theta^{n-1/2}}{r^n} - \frac{3}{2}\frac{v_r^{n-1/2}(v_\theta^{n-1/2})^2}{(r^n)^2}\right]\Delta t + O(\Delta t^2), \tag{40}$$

$$\frac{v_\theta^{n+1/2} - v_\theta^{n-1/2}}{\Delta t} = \frac{q}{m} E_\theta^n - \frac{v_r^{n-1/2} v_\theta^{n-1/2}}{r^n} - \left[\frac{q}{m}\frac{E_\theta^n v_r^{n-1/2}}{r^n} - \frac{(v_r^{n-1/2})^2 v_\theta^{n-1/2}}{(r^n)^2} + \frac{q}{m}\frac{E_r^n v_\theta^{n-1/2}}{r^n} + \frac{(v_\theta^{n-1/2})^3}{2(r^n)^2}\right]\Delta t + O(\Delta t^2). \tag{41}$$

We now expand the new velocities relative to the time step t_n:

$$v_r^{n\pm1/2} = v_r^n \pm \dot{v}_r^n \frac{\Delta t}{2} + \ddot{v}_r^n \frac{\Delta t^2}{8} + O(\Delta t^3) \tag{42}$$

and similarly for v_θ. In Eq. (42), $\dot{v}_r^n = \frac{dv_r}{dt}|_{t=t_n}$. Substitution of Eq. (42) (and its equivalent for v_θ) into Eqs. (40) and (41) leads, after some further algebraic manipulations, to

$$\dot{v}_r^n = \frac{q}{m} E_r^n + \frac{(v_\theta^n)^2}{r^n} + \left[\frac{q}{m}\frac{E_\theta^n v_\theta^n}{r^n} - \frac{1}{2}\frac{v_r^n (v_\theta^n)^2}{r^n}\right]\Delta t + O(\Delta t^2) \tag{43}$$

and

$$\left(1-\frac{v_r^n}{2r^n}\Delta t\right)\dot{v}_\theta^n=\frac{q}{m}E_\theta^n-\frac{v_\theta^n v_r^n}{r^n}-\left[\frac{q}{m}\frac{E_r^n v_\theta^n}{2r^n}+\frac{q}{m}\frac{E_\theta^n v_r^n}{r^n}-\frac{(v_r^n)^2 v_\theta^n}{(r^n)^2}\right]\Delta t+O\left(\Delta t^2\right). \tag{44}$$

Furthermore, Eq. (37) can be further manipulated in similar ways to obtain

$$\dot{r}^{n+1/2}=v_r^{n+1/2}-\frac{(v_\theta^{n+1/2})^2}{2r^{n+1/2}}\Delta t+O\left(\Delta t^2\right). \tag{45}$$

The comparison of Eqs. (11), (14) and (15) with Eqs. (43), (44) and (45) seems to indicate that the Boris numerical algorithm in cylindrical geometry is only first order accurate in time. If this was indeed the case, it would contradict what is reported in the literature [1,4], where the method is claimed to be second order accurate in time. In the next section, we will present an explanation of this apparent puzzle.

4. The Boris mover and its connection with a symmetrized Strang operator splitting method

In order to provide a solution to the puzzle that was presented in Section 3, we start by considering a different method of solution for Eqs. (1) and (2), known as the symmetrized Strang operator splitting algorithm [13]. For an initial value problem of the form

$$\frac{d\mathbf{u}}{dt}=\mathcal{L}(\mathbf{u})=\mathcal{L}_1(\mathbf{u})+\mathcal{L}_2(\mathbf{u}), \tag{46}$$

with initial condition $\mathbf{u}(t=0)=\mathbf{u}_0$, for a given time step the algorithm is as follows:

(1) Solve

$$\frac{d\mathbf{u}^*}{dt}=\mathcal{L}_1\left(\mathbf{u}^*\right) \tag{47}$$

from t^n to $t^{n+1/2}$ with initial condition $\mathbf{u}^*(t^n)=\mathbf{u}^n$.

(2) Solve

$$\frac{d\mathbf{u}^{**}}{dt}=\mathcal{L}_2\left(\mathbf{u}^{**}\right) \tag{48}$$

from t^n to t^{n+1} with initial condition $\mathbf{u}^{**}(t^n)=\mathbf{u}^*(t^{n+1/2})$.

(3) Solve

$$\frac{d\mathbf{u}}{dt}=\mathcal{L}_1(\mathbf{u}) \tag{49}$$

from $t^{n+1/2}$ to t^{n+1} with initial condition $\mathbf{u}(t^{n+1/2})=\mathbf{u}^{**}(t^{n+1})$. The solution sought is $\mathbf{u}(t^{n+1})=\mathbf{u}^{n+1}$.

We note that this scheme is second order accurate in time [13]. With reference to Eqs. (11)–(16), we have $\mathbf{u}=[r,\theta,z,v_r,v_\theta,v_z]^T$. An important point to note is that the symmetrized Strang orbit integrator scheme is not of leap-frog type like the Boris mover: particle velocities and positions are now collocated in time.

Let us choose the splitting operators as

$$\mathcal{L}_1(\mathbf{u})=\frac{q}{m}[0,0,0,E_r+v_\theta B_z-v_z B_\theta,E_\theta-v_r B_z+v_z B_r,E_z+v_r B_\theta-v_\theta B_r]^T \tag{50}$$

and

$$\mathcal{L}_2(\mathbf{u})=\left[v_r,\frac{v_\theta}{r},v_z,\frac{v_\theta^2}{r},-\frac{v_r v_\theta}{r},0\right]^T. \tag{51}$$

That is, the first and last half steps of the Strang splitting algorithm solve for the motion of a particle under the action of the electromagnetic force only, while the intermediate step involves only the inertial forces.

From the perspective of the numerical implementation, it is important to realize that the step of the algorithm involving inertial forces can be completed exactly. In fact, in this case, performing the integration from initial conditions $\mathbf{x}^n$ and $\mathbf{v}^{n*}$, the conservation of angular momentum gives

$$v_\theta(t)=\frac{r^n v_\theta^{n*}}{r(t)}, \tag{52}$$

while the conservation of (kinetic) energy, together with Eqs. (11) and (52) gives

$$r(t)=\sqrt{\left(r^n\right)^2+2r^n v_r^{n*}t+\left[\left(v_r^{n*}\right)^2+\left(v_\theta^{n*}\right)^2\right]t^2}. \tag{53}$$

Eqs. (52) and (53) can be used to solve Eq. (14) (with $\mathbf{E}=\mathbf{B}=0$) to obtain

$$v_r(t)=\frac{r^n v_r^{n*}+[(v_r^{n*})^2+(v_\theta^{n*})^2]t}{r}. \tag{54}$$

Similarly, Eq. (12) leads to

$$\begin{aligned}\theta &= \theta^n+\operatorname{atan}\left(\frac{r^n v_r^{n*}+[(v_r^{n*})^2+(v_\theta^{n*})^2]t}{r^n v_\theta^{n*}}\right)-\operatorname{atan}\left(\frac{v_r^{n*}}{v_\theta^{n*}}\right)\\ &= \theta^n+\operatorname{atan}\left(\frac{v_\theta^{n*}t}{r^n+v_r^{n*}t}\right),\end{aligned} \tag{55}$$

where we have used the property that $\operatorname{atan}\alpha-\operatorname{atan}\beta=\operatorname{atan}\frac{\alpha-\beta}{1+\alpha\beta}$. Eqs. (13) and (16) (with $\mathbf{E}=\mathbf{B}=0$) trivially lead to

$$z(t)=z^n+v_z^{n*}t, \tag{56}$$

$$v_z(t)=v_z^{n*}. \tag{57}$$

Moreover, since the first and last half steps involve only the electromagnetic force, we can reuse the momentum update of the Boris mover.

The Strang operator splitting mover for a given time step corresponding to operators (50) and (51) is summarized as follows:

(1) Half step update (time step $\Delta t/2$) of the velocities with acceleration due to the electromagnetic force only:

$$\mathbf{v}^-=\mathbf{v}^n+\frac{q}{m}\mathbf{E}(\mathbf{x}^n)\frac{\Delta t}{4}, \tag{58}$$

$$\mathbf{v}'=\mathbf{v}^-+f^{n,\Delta t/2}\mathbf{v}^-\times\mathbf{B}(\mathbf{x}^n), \tag{59}$$

$$\mathbf{v}^+=\mathbf{v}^-+\frac{2f^{n,\Delta t/2}}{1+(f^{n,\Delta t/2})^2\mathbf{B}^2}\mathbf{v}'\times\mathbf{B}(\mathbf{x}^n), \tag{60}$$

$$\mathbf{v}^{n*}=\mathbf{v}^++\frac{q}{m}\mathbf{E}(\mathbf{x}^n)\frac{\Delta t}{4}. \tag{61}$$

(2) Full step update (time step Δt) of position and velocities, with acceleration due to inertial forces only:

$$r^{n+1}=\sqrt{(r^n)^2+2r^n v_r^{n*}\Delta t+\left[(v_r^{n*})^2+(v_\theta^{n*})^2\right]\Delta t^2}, \tag{62}$$

$$\theta^{n+1}=\theta^n+\operatorname{atan}\left(\frac{v_\theta^{n*}\Delta t}{r^n+v_r^{n*}\Delta t}\right), \tag{63}$$

$$z^{n+1}=z^n+v_z^{n*}\Delta t, \tag{64}$$

$$v_r^{n**}=\frac{r^n v_r^{n*}+[(v_r^{n*})^2+(v_\theta^{n*})^2]\Delta t}{r^{n+1}}, \tag{65}$$

$$v_\theta^{n**}=\frac{r^n v_\theta^{n*}}{r^{n+1}}, \tag{66}$$

$$v_z^{n**}=v_z^{n*}. \tag{67}$$

(3) Half step update (time step $\Delta t/2$) of the velocities with acceleration due to the electromagnetic force only:

$$\mathbf{v}^-=\mathbf{v}^{n**}+\frac{q}{m}\mathbf{E}(\mathbf{x}^{n+1})\frac{\Delta t}{4}, \tag{68}$$

$$\mathbf{v}'=\mathbf{v}^-+f^{n+1,\Delta t/2}\mathbf{v}^-\times\mathbf{B}(\mathbf{x}^{n+1}), \tag{69}$$

$$\mathbf{v}^+=\mathbf{v}^-+\frac{2f^{n+1,\Delta t/2}}{1+(f^{n+1,\Delta t/2})^2\mathbf{B}^2}\mathbf{v}'\times\mathbf{B}(\mathbf{x}^{n+1}), \tag{70}$$

$$\mathbf{v}^{n+1}=\mathbf{v}^++\frac{q}{m}\mathbf{E}(\mathbf{x}^{n+1})\frac{\Delta t}{4}. \tag{71}$$

It is important to note that, apart from the different notation, Eqs. (19), (20), (21), and (22) and Eqs. (62), (63), (65), and (66) are exactly the same, since the coordinate transformation in the Boris mover in cylindrical geometry is nothing but an exact step in which position and velocity of the particle are updated with the inertial forces only.

We note that the Strang algorithm given by Eqs. (58)–(71) is second order accurate, time reversible, but in general not symplectic.

We now show that two consecutive half steps of the Strang operator splitting algorithm given by Eqs. (58)–(71) can be combined in a single full step without reducing the order of accuracy of the scheme. Let us start from the case without magnetic field. Performing the steps of the algorithm starting from $\mathbf{v}^{n**}$, it is easy to see that

$$\mathbf{v}^{n+1} = \mathbf{v}^{n**} + \frac{q}{m}\mathbf{E}\left(\mathbf{x}^{n+1}\right)\frac{\Delta t}{2},$$
$$\mathbf{v}^{n+1*} = \mathbf{v}^{n+1} + \frac{q}{m}\mathbf{E}\left(\mathbf{x}^{n+1}\right)\frac{\Delta t}{2} = \mathbf{v}^{n**} + \frac{q}{m}\mathbf{E}\left(\mathbf{x}^{n+1}\right)\Delta t. \tag{72}$$

That is, we can combine the last half step of the algorithm at time t^n with the first half step at time t^{n+1} in a single, exact full step with time step Δt. Let us now turn to the case of a finite magnetic field, which for simplicity we consider in the z direction (the proof works just as well in three dimensions). Combining the various steps of the Boris momentum update, one obtains to third order in Δt

$$v_r^{n+1} = v_r^{n**} + \frac{1}{2}\frac{q}{m}\left(E_r^{n+1} + v_\theta^{n**}B_z^{n+1}\right)\Delta t + \frac{1}{8}\frac{q^2}{m^2}B_z^{n+1}\left(E_\theta^{n+1} - v_r^{n**}B_z^{n+1}\right)\Delta t^2$$
$$+ \frac{1}{96}\frac{q^3}{m^3}\left(B_z^{n+1}\right)^2\left\{-3E_r^{n+1} + \left[\left(B_z^{n+1}\right)^2 - 3\right]v_\theta^{n**}B_z^{n+1}\right\}\Delta t^3 + O\left(\Delta t^4\right), \tag{73}$$

$$v_\theta^{n+1} = v_\theta^{n**} + \frac{1}{2}\frac{q}{m}\left(E_\theta^{n+1} - v_r^{n**}B_z^{n+1}\right)\Delta t - \frac{1}{8}\frac{q^2}{m^2}B_z^{n+1}\left(E_r^{n+1} + v_\theta^{n**}B_z^{n+1}\right)\Delta t^2$$
$$- \frac{1}{96}\frac{q^3}{m^3}\left(B_z^{n+1}\right)^2\left\{3E_\theta^{n+1} + \left[\left(B_z^{n+1}\right)^2 - 3\right]v_r^{n**}B_z^{n+1}\right\}\Delta t^3 + O\left(\Delta t^4\right), \tag{74}$$

$$v_z^{n+1} = v_z^{n**} + \frac{q}{m}E_z^{n+1}\frac{\Delta t}{2}, \tag{75}$$

and

$$v_r^{n+1*} = v_r^{n**} + \frac{q}{m}\left(E_r^{n+1} + v_\theta^{n**}B_z^{n+1}\right)\Delta t + \frac{1}{2}\frac{q^2}{m^2}B_z^{n+1}\left(E_\theta^{n+1} - v_r^{n**}B_z^{n+1}\right)\Delta t^2$$
$$+ \frac{1}{48}\frac{q^3}{m^3}\left(B_z^{n+1}\right)^2\left\{-9E_r^{n+1} + \left[\left(B_z^{n+1}\right)^2 - 9\right]v_\theta^{n**}B_z^{n+1}\right\}\Delta t^3 + O\left(\Delta t^4\right), \tag{76}$$

$$v_\theta^{n+1*} = v_\theta^{n**} + \frac{q}{m}\left(E_\theta^{n+1} - v_r^{n**}B_z^{n+1}\right)\Delta t - \frac{1}{2}\frac{q^2}{m^2}B_z^{n+1}\left(E_r^{n+1} + v_\theta^{n**}B_z^{n+1}\right)\Delta t^2$$
$$- \frac{1}{48}\frac{q^3}{m^3}\left(B_z^{n+1}\right)^2\left\{9E_\theta^{n+1} + \left[\left(B_z^{n+1}\right)^2 - 9\right]v_r^{n**}B_z^{n+1}\right\}\Delta t^3 + O\left(\Delta t^4\right), \tag{77}$$

$$v_z^{n+1*} = v_z^{n**} + \frac{q}{m}E_z^{n+1}\Delta t. \tag{78}$$

If one compares Eqs. (76)–(78) with the equivalent expression obtained with a single Δt step starting from $\mathbf{v}^{n**}$ [which correspond to Eqs. (73)–(75) in which $\Delta t \longrightarrow 2\Delta t$], it is easy to see that, in the case where the magnetic field is present, two consecutive half steps with $\Delta t/2$ are not exactly equivalent to a single full step with Δt starting from $\mathbf{v}^{n**}$. However, the important point is that the error between these two procedures is proportional to Δt^3. In other words, for the case with magnetic field, if one decides to substitute the two consecutive half steps with a single full step, the resulting method would still be second order accurate, although it would be different from the symmetrized Strang operator splitting method discussed in this section. This 'new' algorithm can be more computationally efficient than the symmetrized Strang splitting technique described above, since it involves only two steps instead of three and only one force evaluation. This also implies that the algorithm is now formally staggered in time with position and auxiliary velocities that are spaced by a half time step. In fact, it is clear that this 'new' algorithm is nothing but the Boris algorithm in cylindrical geometry described in Section 2.2, which can therefore be interpreted as a Strang operator splitting algorithm that alternates a step with motion due to inertial forces with two half steps combined into a single step where the particle acceleration is due to the Lorentz force.

We note that we could have exchanged the operators (50) and (51) to obtain a different Strang splitting mover alternating half steps with acceleration due to the inertial forces with a full step with acceleration due to the electromagnetic force. Similarly to what discussed above, the two half steps could be combined into a single full step to give rise to a different mover which is still second order accurate.

The Strang algorithm described in this section readily extends to the relativistic case: the first and last steps of the algorithm are equivalent to that of the Boris Cartesian mover and can be treated as described in Ref. [1], while the second step is unchanged in the relativistic case since the magnitude of $\mathbf{v}$ (and the Lorentz factor $\gamma = 1/\sqrt{1 - \mathbf{v}^2/c^2}$, with c the speed of light) is constant. The same considerations are obviously true for the Boris mover in cylindrical geometry.

The connection of the Boris algorithm in cylindrical geometry with a Strang operator splitting method also offers a solution to the puzzle that was presented in Section 3. The reason for the apparent lower accuracy of the algorithm is that the quantities that we have interpreted as velocities at time $n+1/2$ are only zeroth order accurate corrections of the actual velocities or, in other words, are just auxiliary steps used in the Strang algorithm to obtain the actual second order accurate velocities that are defined at time step n. Let us consider the case with $\mathbf{B}=0$ and define

$$\mathbf{v}^n = \frac{\mathbf{v}^{n-1/2} + \mathbf{v}^{n+1/2*}}{2} \tag{79}$$

(where we have kept the notation introduced in Section 2.2). Let us then repeat the analysis on the accuracy of the method with this new insight. From the Taylor expansion of the velocities at time $n+1$ relative to time n, one obtains

$$\begin{aligned} v_r^{n+1} &= v_r^{n+1/2*} + \left[\frac{q}{m}\frac{E_r^n}{2} + \frac{(v_\theta^{n+1/2*})^2}{r^n}\right]\Delta t + \left[-\frac{3}{2}\frac{v_r^{n+1/2*}(v_\theta^{n+1/2*})^2}{(r^n)^2}\right. \\ &\quad \left. + \frac{1}{2}\frac{q}{m}\nabla E_r^n\cdot\mathbf{v}^n\right]\Delta t^2 + O\left(\Delta t^3\right), \end{aligned} \tag{80}$$

$$\begin{aligned} v_\theta^{n+1} &= v_\theta^{n+1/2*} + \left[\frac{q}{m}\frac{E_\theta^n}{2} - \frac{v_r^{n+1/2*}v_\theta^{n+1/2*}}{r^n}\right]\Delta t + \left[-\frac{1}{2}\frac{(v_\theta^{n+1/2*})^3}{(r^n)^2}\right. \\ &\quad \left. + \frac{(v_r^{n+1/2*})^2 v_\theta^{n+1/2*}}{(r^n)^2} + \frac{1}{2}\frac{q}{m}\nabla E_\theta^n\cdot\mathbf{v}^n\right]\Delta t^2 + O\left(\Delta t^3\right), \end{aligned} \tag{81}$$

which can be expressed as

$$\begin{aligned} v_r^{n+1} &= v_r^n + \left[\frac{q}{m}E_r^n + \frac{(v_\theta^n)^2}{r^n}\right]\Delta t + \left[-\frac{3}{2}\frac{v_r^n(v_\theta^n)^2}{(r^n)^2}\right. \\ &\quad \left. + \frac{1}{2}\frac{q}{m}\nabla E_r^n\cdot\mathbf{v}^n + \frac{q}{m}\frac{E_\theta^n v_\theta^n}{r^n}\right]\Delta t^2 + O\left(\Delta t^3\right), \\ v_\theta^{n+1} &= v_\theta^n + \left[\frac{q}{m}E_\theta^n - \frac{v_r^n v_\theta^n}{r^n}\right]\Delta t + \left[-\frac{1}{2}\frac{(v_\theta^n)^3}{(r^n)^2}\right. \\ &\quad \left. + \frac{(v_r^n)^2 v_\theta^n}{(r^n)^2} + \frac{1}{2}\frac{q}{m}\nabla E_\theta^n\cdot\mathbf{v}^n - \frac{q}{m}\frac{E_\theta^n v_r^n + E_r^n v_\theta^n}{2r^n}\right]\Delta t^2 + O\left(\Delta t^3\right), \end{aligned} \tag{82}$$

since

$$v_{r,\theta}^{n+1/2*} = v_{r,\theta}^n + \frac{q}{m}\frac{E_{r,\theta}^n}{2}\Delta t. \tag{83}$$

Similarly, one can Taylor expand the velocities at time $n-1$ relative to time n:

$$\begin{aligned} v_r^{n-1} &= v_r^n - \left[\frac{q}{m}E_r^n + \frac{(v_\theta^n)^2}{r^n}\right]\Delta t + \left[-\frac{3}{2}\frac{v_r^n(v_\theta^n)^2}{(r^n)^2}\right. \\ &\quad \left. + \frac{1}{2}\frac{q}{m}\nabla E_r^n\cdot\mathbf{v}^n + \frac{q}{m}\frac{E_\theta^n v_\theta^n}{r^n}\right]\Delta t^2 + O\left(\Delta t^3\right), \\ v_\theta^{n-1} &= v_\theta^n - \left[\frac{q}{m}E_\theta^n - \frac{v_r^n v_\theta^n}{r^n}\right]\Delta t + \left[-\frac{1}{2}\frac{(v_\theta^n)^3}{(r^n)^2}\right. \\ &\quad \left. + \frac{(v_r^n)^2 v_\theta^n}{(r^n)^2} + \frac{1}{2}\frac{q}{m}\nabla E_\theta^n\cdot\mathbf{v}^n - \frac{q}{m}\frac{E_\theta^n v_r^n + E_r^n v_\theta^n}{2r^n}\right]\Delta t^2 + O\left(\Delta t^3\right). \end{aligned} \tag{84}$$

From Eqs. (82) and (84) it is easy to recover the second order accuracy of the scheme:

$$\begin{aligned} \frac{v_r^{n+1} - v_r^{n-1}}{2\Delta t} &= \left.\frac{dv_r}{dt}\right|_{t=t^n} + O\left(\Delta t^2\right) = \frac{q}{m}E_r^n + \frac{(v_\theta^n)^2}{r^n} + O\left(\Delta t^2\right), \\ \frac{v_\theta^{n+1} - v_\theta^{n-1}}{2\Delta t} &= \left.\frac{dv_\theta}{dt}\right|_{t=t^n} + O\left(\Delta t^2\right) = \frac{q}{m}E_\theta^n - \frac{v_r^n v_\theta^n}{r^n} + O\left(\Delta t^2\right). \end{aligned} \tag{85}$$

Obviously the same analysis could have been conducted around time $n+1/2$ leading to the same result if one defines

$$\hat{\mathbf{v}}^{n+1/2} = \frac{\mathbf{v}^{n+1} + \mathbf{v}^n}{2}, \tag{86}$$

which is second order accurate in time, unlike the velocities defined in Section 2.2. For instance, the Taylor expansion of $\hat{v}_r^{n+1/2}$ relative to time n yields

$$\hat{v}_r^{n+1/2} = \frac{v_r^{n+1}+v_r^n}{2} = v_r^n + \left[\frac{(v_\theta^n)^2}{r^n} + \frac{q}{m}E_r^n\right]\frac{\Delta t}{2} + O\left(\Delta t^2\right), \tag{87}$$

which can be substituted in the following equation

$$\begin{aligned}\frac{r^{n+1}-r^n}{\Delta t} &= \left.\frac{dr}{dt}\right|_{t^{n+1/2}} + O\left(\Delta t^2\right) = v_r^n + \left[\frac{(v_\theta^n)^2}{r^n} + \frac{q}{m}E_r^n\right]\frac{\Delta t}{2} + O\left(\Delta t^2\right)\\ &= \hat{v}_r^{n+1/2} + O\left(\Delta t^2\right),\end{aligned} \tag{88}$$

to recover second order accuracy.

If one compares Eq. (87) with the expansion of $v_r^{n+1/2}$, rearranged as

$$v_r^{n+1/2} = v_r^n + \left[\frac{(v_\theta^n)^2}{r^n} + \frac{q}{m}\frac{E_r^n}{2}\right]\Delta t + \left[\frac{q}{m}\frac{v_\theta^n E_\theta^n}{r^n} - \frac{3}{2}\frac{v_r^n (v_\theta^n)^2}{(r^n)^2}\right]\Delta t^2 + O\left(\Delta t^3\right), \tag{89}$$

one can see that the error in $v_r^{n+1/2}$ is proportional to Δt.

Before we conclude our analysis of accuracy, we need to consider the initial half step of the algorithm. We do it in the next subsection.

4.1. Initial half step of the Boris mover in cylindrical geometry

The analysis conducted in Section 3 in Cartesian geometry reminded us that care must be taken in choosing the initial half step of the leap-frog/Boris algorithm: in Cartesian geometry, the initial half step bear the (rather modest) requirement of being at least first order accurate in order for the overall scheme to retain second order accuracy. For cylindrical geometry, the connection between the Boris algorithm and a symmetrized Strang operator splitting method discussed in Section 4 already tells us how to choose the initial half step for a second order accurate scheme. However, it is instructive to study how different choices of the first half step affect the overall accuracy of the scheme and this is done in this section.

Starting from an initial condition in terms of r^0 and $\mathbf{v}^0$, let us begin by assuming that $\mathbf{v}^{-1/2}$ can be obtained somehow and explicitate the first step of the Boris algorithm:

$$\begin{aligned}
&v_{r,\theta}^{1/2*} = v_{r,\theta}^{-1/2} + \frac{q}{m}E_{r,\theta}^0\Delta t,\\
&r^1 = \sqrt{\left(r^0 + v_r^{1/2*}\Delta t\right)^2 + \left(v_\theta^{1/2*}\Delta t\right)^2},\\
&v_r^{1/2} = \frac{r^0 + v_r^{1/2*}\Delta t}{r^1}v_r^{1/2*} + \frac{v_\theta^{1/2*}\Delta t}{r^1}v_\theta^{1/2*},\\
&v_\theta^{1/2} = -\frac{v_\theta^{1/2*}\Delta t}{r^1}v_r^{1/2*} + \frac{r^0 + v_r^{1/2*}\Delta t}{r^1}v_\theta^{1/2*},\\
&v_{r,\theta}^{3/2*} = v_{r,\theta}^{1/2} + \frac{q}{m}E_{r,\theta}^1\Delta t,\\
&v_{r,\theta}^1 = \frac{v_{r,\theta}^{1/2} + v_{r,\theta}^{3/2*}}{2}.
\end{aligned} \tag{90}$$

The Taylor expansion of the quantities at time $t=\Delta t$ relative to time $t=0$ is

$$\begin{aligned}v_r^1 &= v_r^{-1/2} + \left[\frac{3}{2}\frac{q}{m}E_r^0 + \frac{(v_\theta^{-1/2})^2}{r^0}\right]\Delta t + \left[-\frac{3}{2}\frac{v_r^{-1/2}(v_\theta^{-1/2})^2}{(r^0)^2} + 2\frac{q}{m}\frac{E_\theta^0 v_\theta^{-1/2}}{r^0} + \frac{1}{2}\frac{q}{m}\nabla E_r^0\cdot\mathbf{v}^0\right]\Delta t^2\\ &\quad + O\left(\Delta t^3\right),\end{aligned} \tag{91}$$

$$\begin{aligned}v_\theta^1 &= v_\theta^{-1/2} + \left[\frac{3}{2}\frac{q}{m}E_\theta^0 - \frac{v_r^{-1/2}v_\theta^{-1/2}}{r^0}\right]\Delta t + \left[-\frac{(v_\theta^{-1/2})^3}{2(r^0)^2} + \frac{(v_r^{-1/2})^2 v_\theta^{-1/2}}{(r^0)^2}\right.\\ &\quad \left. - \frac{q}{m}\frac{E_r^0 v_\theta^{-1/2} + E_\theta^0 v_r^{-1/2}}{r^0} + \frac{1}{2}\frac{q}{m}\nabla E_\theta^0\cdot\mathbf{v}^0\right]\Delta t^2 + O\left(\Delta t^3\right),\end{aligned} \tag{92}$$

$$r^1 = r^0 + v_r^{-1/2}\Delta t + \left[\frac{q}{m}E_r^0 + \frac{(v_\theta^{-1/2})^2}{2r^0}\right]\Delta t^2 + O\left(\Delta t^3\right). \tag{93}$$

We repeat the analysis of Section 3. We can calculate analytically the expansion of the velocities at time $t = \Delta t$ from the model equations (11)–(16):

$$v_r^1 = v_r^0 + \left[\frac{q}{m}E_r^0 + \frac{(v_\theta^0)^2}{r^0}\right]\Delta t + \left[\frac{q}{m}\nabla E_r^0\cdot\mathbf{v}^0 + 2\frac{q}{m}\frac{E_\theta^0 v_\theta^0}{r^0} - 3\frac{v_r^0(v_\theta^0)^2}{(r^0)^2}\right]\frac{\Delta t^2}{2} + O\left(\Delta t^3\right), \tag{94}$$

$$v_\theta^1 = v_\theta^0 + \left[\frac{q}{m}E_\theta^0 - \frac{v_r^0 v_\theta^0}{r^0}\right]\Delta t + \left[\frac{q}{m}\nabla E_\theta^0\cdot\mathbf{v}^0 - \frac{q}{m}\frac{E_\theta^0 v_r^0 + E_r^0 v_\theta^0}{r^0} - \frac{(v_\theta^0)^3}{(r^0)^2} + 2\frac{(v_r^0)^2 v_\theta^0}{(r^0)^2}\right]\frac{\Delta t^2}{2} + O\left(\Delta t^3\right), \tag{95}$$

$$r^1 = r^0 + v_r^0\Delta t + \left[\frac{q}{m}E_r^0 + \frac{(v_\theta^0)^2}{r^0}\right]\frac{\Delta t^2}{2} + O\left(\Delta t^3\right), \tag{96}$$

and compare with the ones obtained from the algorithm, Eqs. (91)–(93). First, let us consider the case $v_r^{-1/2} = v_r^0$ and $v_\theta^{-1/2} = v_\theta^0$ and substitute in Eqs. (91)–(93). A comparison with Eqs. (94)–(96) indicates that the error is proportional to Δt. This is the same as for the Cartesian case discussed in Section 3. Let us now try a more accurate expression for $\mathbf{v}^{-1/2}$,

$$v_r^{-1/2} = v_r^0 - \left[\frac{q}{m}E_r^0 + \frac{(v_\theta^0)^2}{r^0}\right]\frac{\Delta t}{2},$$
$$v_\theta^{-1/2} = v_\theta^0 - \left[\frac{q}{m}E_\theta^0 - \frac{v_r^0 v_\theta^0}{r^0}\right]\frac{\Delta t}{2}, \tag{97}$$

and substitute into Eqs. (91)–(93) to obtain

$$v_r^1 = v_r^0 + \left[\frac{q}{m}E_r^0 + \frac{(v_\theta^0)^2}{2r^0}\right]\Delta t + \left[-\frac{v_r^0(v_\theta^0)^2}{(r^0)^2} + 2\frac{q}{m}\frac{E_\theta^0 v_\theta^0}{r^0} + \frac{q}{m}\nabla E_r^0\cdot\mathbf{v}^0\right]\frac{\Delta t^2}{2} + O\left(\Delta t^3\right), \tag{98}$$

$$v_\theta^1 = v_\theta^0 + \left[\frac{q}{m}E_\theta^0 - \frac{v_r^0 v_\theta^0}{2r^0}\right]\Delta t + \left[\frac{(v_r^0)^2 v_\theta^0}{(r^0)^2} - \frac{q}{m}\frac{E_r^0 v_\theta^0 + E_\theta^0 v_r^0}{r^0} + \frac{q}{m}\nabla E_\theta^0\cdot\mathbf{v}^0\right]\frac{\Delta t^2}{2} + O\left(\Delta t^3\right), \tag{99}$$

$$r^1 = r^0 + v_r^0\Delta t + \frac{q}{m}\frac{E_r^0}{2}\Delta t^2 + O\left(\Delta t^3\right). \tag{100}$$

The comparison of Eqs. (98)–(100) with Eqs. (94)–(96) indicates that the error for the velocities is still proportional to Δt and thus the overall accuracy of the scheme is still first order. Obviously, further higher order approximations to $\mathbf{v}^{-1/2}$ still yield the same result. In fact, the only way to obtain second order accuracy of the scheme, which is obvious if we recognize the connection of the Boris algorithm in cylindrical geometry with a Strang operator splitting method, is to perform the initial half step with only the electromagnetic force. That is:

$$v_r^{-1/2} = v_r^0 - \frac{q}{m}E_r^0\frac{\Delta t}{2},$$
$$v_\theta^{-1/2} = v_\theta^0 - \frac{q}{m}E_\theta^0\frac{\Delta t}{2}. \tag{101}$$

Again, the heart of the matter is that it is incorrect to interpret the velocities $\mathbf{v}^{n+1/2}$ in the Boris algorithm in cylindrical geometry as the second order accurate velocities at time $t^{n+1/2}$.

5. Numerical results

In this section, we verify the accuracy of the Boris mover in cylindrical geometry with a numerical study. As a test case, we consider a system where a charged, spherical dust grain of charge Q_d and radius $\rho_1 = 1$ is surrounded by vacuum. The domain of interest is enclosed by an outer sphere of radius $\rho_2 = 10$ and by the dust grain. The charged dust grain gives rise to the following electric field

$$E_r(r,\theta,z) = \frac{Q_d}{2}\frac{r}{\sqrt{r^2+z^2}}, \tag{102}$$

$$E_\theta(r,\theta,z) = 0, \tag{103}$$

$$E_z(r,\theta,z) = \frac{Q_d}{2}\frac{z}{\sqrt{r^2+z^2}}. \tag{104}$$

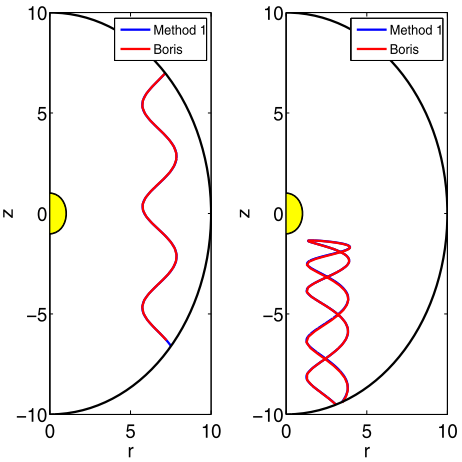

Fig. 2. Particle trajectories in (r, z) space obtained with Method 1 (blue line) and with the Boris method (red line, $\Delta t = 0.2$) for test particles 1 and 2. The injection parameters for each particle are discussed in the caption of Tables 1 and 2. The initial half step $\mathbf{v}^{-1/2}$ in the Boris method is given by a first order backward half step based only on the electromagnetic force. (For interpretation of the references to color in this figure, the reader is referred to the web version of this article.)

In addition, we impose a constant magnetic field in the z direction: $\mathbf{B} = (0, 0, 2)$. We inject particles at random positions on the outer boundary, with random injection velocities, and follow their trajectory into the system. This test case is representative of typical simulations of charging and shielding of objects immersed in a plasma, as done for instance in Refs. [14–18]. We compare several methods. The first, labeled as 'Method 1', solves Eqs. (11)–(16) with a Matlab adaptive ODE solver with extremely high resolution (with relative and absolute tolerances equal to $\mathrm{tol} = 10^{-13}$ and maximum step size equal to $\Delta t^{\max} = 5 \times 10^{-4}$). For the second method, we apply the Boris mover algorithm in cylindrical geometry (labeled as 'Boris' in the following) outlined in Section 2.2. For practical purposes, Method 1 provides the equivalent of an analytic solution and comparing it with the Boris method with different values of the time step allows to test the accuracy of the latter. We have also implemented numerically the Strang operator splitting method detailed in Section 4. Moreover, we introduce four measures of error

$$\mathrm{Err}_1 = \sqrt{\sum_n \left| r^n_{\text{Method 1}} - r^n \right|^2 \Delta t}, \tag{105}$$

$$\mathrm{Err}_2 = \sqrt{\sum_n \left| z^n_{\text{Method 1}} - z^n \right|^2 \Delta t}, \tag{106}$$

$$\mathrm{Err}_3 = \sqrt{\sum_n \left| v^n_{r\,\text{Method 1}} - v^n_r \right|^2 \Delta t}, \tag{107}$$

$$\mathrm{Err}_4 = \sqrt{\sum_n \left| v^n_{z\,\text{Method 1}} - v^n_z \right|^2 \Delta t}, \tag{108}$$

where $\mathbf{x}^n$ and $\mathbf{v}^n$ are obtained by one of the methods described in the paper. For the Boris method, the velocities at time n are given by Eq. (79).

We have followed the trajectories of several test particles randomly injected from the outer boundary. We have fixed $q = -1$ (i.e. electrons), $m = 1$ and $Q_d = -10$ (i.e. negatively charged dust grain). A test particle is followed until it returns to the outer boundary or is absorbed by the dust grain at the inner boundary. Therefore the final time of the simulation, T, varies with the test particle injection parameters. Fig. 2 shows the trajectory of two representative test particles obtained with Method 1 (blue line) and the Boris algorithm (red line, $\Delta t = 0.2$). The initial half step of the Boris algorithm to obtain $\mathbf{v}^{-1/2}$ is obtained by a first order backward half step with acceleration given only by the electromagnetic force. The first test particle (Fig. 2, left) has the following injection parameters: $r = 7.16$, $z = 6.98$, $v_r = -1.91$, $v_\theta = 0.90$, $v_z = -1.71$. It moves relatively far away from the dust grain and along the magnetic field with the typical gyromotion in the direction perpendicular to the magnetic field. It exits the system at time $T = 8.37$, roughly symmetrically relative to the injection point. The second test particle (Fig. 2, right) has the following injection parameters: $r = 3.09$, $z = -9.51$, $v_r = -2.06$, $v_\theta = 1.54$, $v_z = 1.55$. It moves closer to the dust grain and feels a strong electrostatic repulsion, such that it reverses its direction of motion along the magnetic field and exits near the injection point. Fig. 3 shows the same particle trajectories as in Fig. 2 but now $\mathbf{v}^{-1/2}$ for the Boris algorithm is obtained with Method 1 (thus including also inertial forces in the first half step). It is clear from Fig. 3 that now the Boris method with $\Delta t = 0.2$ does not capture accurately the trajectory of

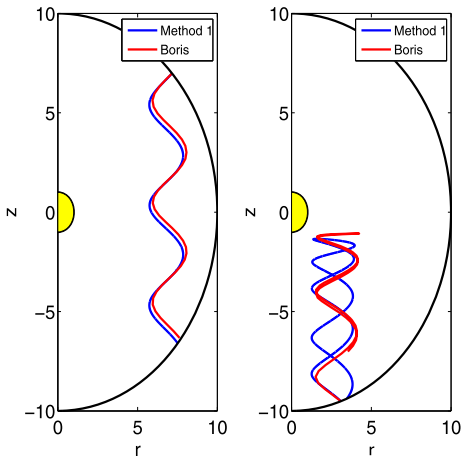

Fig. 3. Particle trajectories in (r, z) space obtained with Method 1 (blue line) and with the Boris method (red line, $\Delta t = 0.2$) for test particles 1 and 2. The injection parameters for each particle are discussed in the caption of Tables 1 and 2. The initial half step $\mathbf{v}^{-1/2}$ in the Boris method is given by Method 1 and includes both electromagnetic and inertial forces. (For interpretation of the references to color in this figure, the reader is referred to the web version of this article.)

Table 1
Test particle 2, Boris method with $\mathbf{v}^{-1/2}$ given by a first order backward half step including only the electromagnetic force. Injection parameters: $r = 3.09$, $z = -9.51$, $v_r = -2.06$, $v_\theta = 1.54$, $v_z = 1.55$. Comparison of the error measures from Eqs. (105)–(108) changing the time step in Boris' method. The total time of the simulation is $T = 15.80$, while the maximum time step of the simulation performed with Method 1 is $\Delta t = 1.25 \times 10^{-4}$.

Δt	Err_1	Err_2	Err_3	Err_4
0.2	3.92×10^{-2}	1.16×10^{-1}	1.57×10^{-1}	2.08×10^{-2}
0.1	9.74×10^{-3}	2.88×10^{-2}	3.95×10^{-2}	5.18×10^{-3}
0.05	2.43×10^{-3}	7.17×10^{-3}	9.88×10^{-3}	1.29×10^{-3}
0.025	6.08×10^{-4}	1.79×10^{-3}	2.47×10^{-3}	3.23×10^{-4}
0.0125	1.52×10^{-4}	4.47×10^{-4}	6.18×10^{-4}	8.09×10^{-5}
0.00625	3.80×10^{-5}	1.12×10^{-4}	1.55×10^{-4}	2.02×10^{-5}

Table 2
Test particle 2, Boris method with $\mathbf{v}^{-1/2}$ given by Method 1 (namely including both electromagnetic and inertial forces). Injection parameters: $r = 3.09$, $z = -9.51$, $v_r = -2.06$, $v_\theta = 1.54$, $v_z = 1.55$. Comparison of the error measures from Eqs. (105)–(108) changing the time step in Boris' method. The total time of the simulation is $T = 15.80$, while the maximum time step of the simulation performed with Method 1 is $\Delta t = 1.25 \times 10^{-4}$.

Δt	Err_1	Err_2	Err_3	Err_4
0.2	1.38×10^{0}	4.54×10^{0}	1.99×10^{0}	7.87×10^{-1}
0.1	6.75×10^{-1}	1.94×10^{0}	1.00×10^{0}	3.27×10^{-1}
0.05	3.35×10^{-1}	9.26×10^{-1}	5.02×10^{-1}	1.57×10^{-1}
0.025	1.67×10^{-1}	4.56×10^{-1}	2.51×10^{-1}	7.74×10^{-2}
0.0125	8.32×10^{-2}	2.27×10^{-1}	1.25×10^{-1}	3.85×10^{-2}
0.00625	4.16×10^{-2}	1.13×10^{-1}	6.27×10^{-2}	1.92×10^{-2}

these particles, particularly for the second test particle. Similar conclusions can be drawn from Tables 1 and 2, which report a convergence study of the error measures (105)–(108) changing the time step of the Boris method, for the second test particle. Tables 1, 2 corresponds to the case of Figs. 2, 3. In Table 2, for instance, the errors are of order unity for $\Delta t = 0.2$, about 40 times larger than the corresponding errors in Table 1. Most important, the convergence study confirms the findings of Section 4: the Boris mover in cylindrical geometry is second order accurate only if one starts the algorithm with a first order backward half step involving only the electromagnetic force: asymptotically, by decreasing the time step by a factor of two, the errors decrease by a factor of four. On the other hand, an accurate representation of $\mathbf{v}^{-1/2}$ (which includes also the inertial forces) gives a scheme that is only first order accurate. The error measures Err_1 and Err_3 for Tables 1 and 2 are plotted in Fig. 4.

Table 3 shows a convergence study changing the time step of the simulation for test particle 2, using the Strang splitting method. As expected, one can see from Table 3 that the errors decrease quadratically as the time step is divided by two. As we argued in Section 4, the Boris and Strang methods are not exactly equivalent for finite magnetic field. One could expect the Boris algorithm to be faster since it involves only two steps instead of three, but the Strang method could be more accurate since it does a better sampling of the particle trajectory. Therefore the actual comparison between the two methods should be assessed for the same accuracy. By taking the ratios of the respective entries in Tables 1 and 3, one can see that the errors are comparable (within 30%) for three error measures out of four, while Err_3 for the Boris algorithm

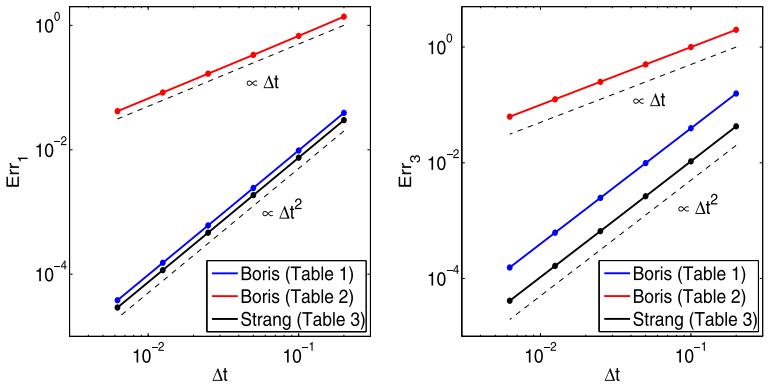

Fig. 4. Error measures Err_1 and Err_3 versus Δt for Tables 1, 2 and 3.

Table 3
Test particle 2, Strang operator splitting method of Section 4. Comparison of the error measures from Eqs. (105)–(108) changing the time step in the Strang method. Other parameters are the same as in Table 1.

Δt	Err_1	Err_2	Err_3	Err_4
0.2	2.99×10^{-2}	1.03×10^{-1}	4.26×10^{-2}	1.86×10^{-2}
0.1	7.44×10^{-3}	2.55×10^{-2}	1.06×10^{-2}	4.63×10^{-3}
0.05	1.86×10^{-3}	6.36×10^{-3}	2.64×10^{-3}	1.15×10^{-3}
0.025	4.64×10^{-4}	1.59×10^{-3}	6.58×10^{-4}	2.89×10^{-4}
0.0125	1.16×10^{-4}	3.97×10^{-4}	1.65×10^{-4}	7.21×10^{-5}
0.00625	2.90×10^{-5}	9.92×10^{-5}	4.12×10^{-5}	1.80×10^{-5}

is about 3.7 times larger. The same trend is also valid for test particle 1 (not shown). By studying several random test particles, we have not found a general trend that favors the Strang method for all the error measures. However, with our C implementation of both algorithms, the Boris mover is $\sim 20\%$ faster and should be preferred.

We have also checked the performance of the Strang mover obtained by interchanging the operators (50) and (51). This alternative Strang mover combines half steps with acceleration due to the inertial forces with a full step with acceleration due to the electromagnetic force. From an accuracy point of view, we have not found a general trend indicating that this way of splitting operators is any better. However, with our C implementation, it is about $\sim 25\%$ slower than the Strang algorithm of Section 4. The Boris mover remains faster than both Strang algorithms.

6. The case of uniform and static magnetic field: cyclotronic mover in cylindrical geometry

In the case of uniform and static magnetic field the steps of the Strang splitting method can be combined differently to obtain a more efficient algorithm. The idea was put forward in Cartesian geometry in Ref. [5], where it was labeled as the cyclotronic mover, and is discussed here in the context of cylindrical geometry. This method is symplectic and therefore time reversible. For simplicity, we consider a constant magnetic field directed along z.

Relative to Section 4, the operator splitting technique is modified as follows: in the half steps, particles are accelerated due to inertial forces and due to the magnetic part of the Lorentz force, while the intermediate full step includes only acceleration due to the electric field. In other words, the operators introduced in Section 4 become

$$\mathcal{L}_1(\mathbf{u}) = \left[v_r, \frac{v_\theta}{r}, v_z, \frac{v_\theta^2}{r} + \frac{q}{m} v_\theta B_z, -\frac{v_r v_\theta}{r} - \frac{q}{m} v_r B_z, 0 \right]^T \tag{109}$$

and

$$\mathcal{L}_2(\mathbf{u}) = \frac{q}{m} [0, 0, 0, E_r, E_\theta, E_z]^T. \tag{110}$$

The advantage of this technique is that the half steps remain still completely analytical. Following the analysis of Section 4, it is well known that a particle moving in a constant magnetic field conserves the canonical angular momentum:

$$r v_\theta + \frac{\omega r^2}{2} = \mathcal{P}_\theta \tag{111}$$

and the kinetic energy perpendicular to the magnetic field:

$$\frac{v_r^2 + v_\theta^2}{2} = \mathcal{E}. \tag{112}$$

Thus, Eq. (14) (with $\mathbf{E} = B_r = B_\theta = 0$) can be rewritten as

$$\frac{d^2 r^2}{dt^2} = 4\mathcal{E} + 2\omega\mathcal{P}_\theta - \omega^2 r^2, \tag{113}$$

where we have introduced the cyclotron frequency $\omega = qB_z/m$. Finally, from the solution of Eq. (113), it is easy to obtain

$$r = \sqrt{\left(r^n\right)^2 \cos(\omega t) + \frac{4\mathcal{E}^n + 2\omega\mathcal{P}_\theta^n}{\omega^2}\left[1 - \cos(\omega t)\right] + 2\frac{r^n v_r^n}{\omega}\sin(\omega t)}, \tag{114}$$

$$v_r = \frac{1}{r}\left[r^n v_r^n \cos(\omega t) - \frac{\omega (r^n)^2}{2}\sin(\omega t) + \frac{2\mathcal{E}^n + \omega\mathcal{J}^n}{\omega}\sin(\omega t)\right], \tag{115}$$

and, from Eq. (111),

$$v_\theta = \frac{\mathcal{P}_\theta^n}{r} - \frac{\omega}{2} r. \tag{116}$$

In Eqs. (114)–(116), we have performed the integration from $t = t^n$ and labeled the symbols accordingly. Thus, the cyclotronic mover in cylindrical geometry, analogue of that of Ref. [5], is

(1) Half step update (time step $\Delta t/2$) of positions and velocities with acceleration due to inertial forces and the magnetic part of the Lorentz force:

$$r^{n*} = \sqrt{\left(r^n\right)^2 \cos\left(\omega\frac{\Delta t}{2}\right) + \frac{4\mathcal{E}^n + 2\omega\mathcal{P}_\theta^n}{\omega^2}\left[1 - \cos\left(\omega\frac{\Delta t}{2}\right)\right] + 2\frac{r^n v_r^n}{\omega}\sin\left(\omega\frac{\Delta t}{2}\right)}, \tag{117}$$

$$\theta^{n*} = \theta^n - \frac{\omega\Delta t}{4} + \frac{2\mathcal{P}_\theta^n \omega}{\alpha^n}\left\{\operatorname{atanh}\left(\frac{2r^n v_r^n \omega}{\alpha^n}\right) - \operatorname{atanh}\left[2\frac{r^n v_r^n \omega}{\alpha^n} + \frac{8\mathcal{E}^n + 4\omega\mathcal{P}_\theta^n - \omega^2 (r^n)^2}{\alpha^n}\tan\left(\frac{\omega\Delta t}{4}\right)\right]\right\}, \tag{118}$$

$$z^{n*} = z^n + v_z^n\frac{\Delta t}{2}, \tag{119}$$

$$v_r^{n*} = \frac{1}{r^{n*}}\left[r^n v_r^n \cos\left(\omega\frac{\Delta t}{2}\right) - \frac{\omega (r^n)^2}{2}\sin\left(\omega\frac{\Delta t}{2}\right) + \frac{2\mathcal{E}^n + \omega\mathcal{P}_\theta^n}{\omega}\sin\left(\omega\frac{\Delta t}{2}\right)\right], \tag{120}$$

$$v_\theta^{n*} = \frac{\mathcal{P}_\theta^n}{r^{n*}} - \frac{\omega}{2} r^{n*}, \tag{121}$$

$$v_z^{n*} = v_z^n, \tag{122}$$

where

$$\alpha^n = \sqrt{\omega^2\left(r^n\right)^2\left[4\left(v_r^n\right)^2 - \left(8\mathcal{E}^n + 4\omega\mathcal{P}_\theta^n\right) + \omega^2\left(r^n\right)^2\right]}. \tag{123}$$

(2) Full step update (time step Δt) of the velocities only, with acceleration due to the electric field:

$$\mathbf{v}^{n**} = \mathbf{v}^{n*} + \frac{q}{m}\mathbf{E}\left(\mathbf{x}^{n*}\right)\Delta t. \tag{124}$$

(3) Half step update (time step $\Delta t/2$) of positions and velocities with acceleration due to inertial forces and the magnetic part of the Lorentz force:

$$r^{n+1} = \sqrt{\left(r^{n*}\right)^2 \cos\left(\omega\frac{\Delta t}{2}\right) + \frac{4\mathcal{E}^{n**} + 2\omega\mathcal{P}_\theta^{n**}}{\omega^2}\left[1 - \cos\left(\omega\frac{\Delta t}{2}\right)\right] + 2\frac{r^{n*} v_r^{n**}}{\omega}\sin\left(\omega\frac{\Delta t}{2}\right)}, \tag{125}$$

$$\theta^{n+1} = \theta^{n*} - \frac{\omega\Delta t}{4} + \frac{2\mathcal{P}_\theta^{n**}\omega}{\alpha^{n**}}\left\{\operatorname{atanh}\left(\frac{2r^{n*} v_r^{n**}\omega}{\alpha^{n**}}\right) - \operatorname{atanh}\left[2\frac{r^{n*} v_r^{n**}\omega}{\alpha^{n**}} + \frac{8\mathcal{E}^{n**} + 4\omega\mathcal{P}_\theta^{n**} - \omega^2 (r^{n*})^2}{\alpha^{n**}}\tan\left(\frac{\omega\Delta t}{4}\right)\right]\right\}, \tag{126}$$

$$z^{n+1} = z^{n*} + v_z^{n**}\frac{\Delta t}{2}, \tag{127}$$

$$v_r^{n+1} = \frac{1}{r^{n+1}}\left[r^{n*} v_r^{n**}\cos\left(\omega\frac{\Delta t}{2}\right) - \frac{\omega (r^{n*})^2}{2}\sin\left(\omega\frac{\Delta t}{2}\right) + \frac{2\mathcal{E}^{n**} + \omega\mathcal{P}_\theta^{n**}}{\omega}\sin\left(\omega\frac{\Delta t}{2}\right)\right], \tag{128}$$

Table 4
Test particle 2, leap-frog cyclotronic mover. Injection parameters: $r = 3.09$, $z = -9.51$, $v_r = -2.06$, $v_\theta = 1.54$, $v_z = 1.55$. Comparison of the error measures from Eqs. (105)–(108) changing the time step in the leap-frog cyclotronic mover. The total time of the simulation is $T = 15.80$, while the maximum time step of the simulation performed with Method 1 is $\Delta t = 1.25 \times 10^{-4}$.

Δt	Err_1	Err_2	Err_3	Err_4
0.2	4.10×10^{-3}	3.33×10^{-2}	5.30×10^{-3}	7.33×10^{-3}
0.1	1.02×10^{-3}	8.18×10^{-3}	1.29×10^{-3}	1.81×10^{-3}
0.05	2.53×10^{-4}	2.03×10^{-3}	3.20×10^{-4}	4.52×10^{-4}
0.025	6.33×10^{-5}	5.08×10^{-4}	7.98×10^{-5}	1.13×10^{-4}
0.0125	1.58×10^{-5}	1.27×10^{-4}	1.99×10^{-5}	2.82×10^{-5}
0.00625	3.95×10^{-6}	3.17×10^{-5}	4.98×10^{-6}	7.05×10^{-6}

$$v_\theta^{n+1} = \frac{\mathcal{P}_\theta^{n**}}{r^{n+1}} - \frac{\omega}{2} r^{n+1}, \tag{129}$$

$$v_z^{n+1} = v_z^{n**}. \tag{130}$$

The scheme is still second order accurate in time and symplectic (therefore time reversible). Moreover, it readily extends to the relativistic case: the first and last steps of the algorithm are characterized by constant Lorentz factor γ (since the magnetic field does not perform work and the kinetic energy is conserved), while the update due to the electric field can be treated as in the Cartesian Boris scheme. However, the important point is that the gyration motion perpendicular to the magnetic field is decoupled from the rest of the dynamics. As pointed out in Ref. [5], this has important consequences from the perspective of explicit electrostatic PIC simulations of strongly magnetized plasmas. Explicit PIC methods must resolve the fastest frequency and the shortest length scale in the system for stability reasons [1]. This can easily be the gyromotion when the plasma is strongly magnetized and impose stringent constraints on the time step of the simulation. The cyclotronic integrator, on the other hand, relaxes these constraints since the gyromotion is solved analytically. Ref. [5] reports results showing a factor of up to 10 gain of the cyclotronic mover relative to the classic Boris mover.

For the application to PIC, Patacchini and Hutchinson [5] have proposed a slight modification of the cyclotronic mover where two consecutive half steps are concatenated and substituted by a single full step with time step Δt. In practice this makes the algorithm of leap-frog type, and we will refer to it as the leap-frog cyclotronic mover. This procedure is not exact, but the resulting scheme remains second order accurate and symplectic, and is more computationally efficient (similarly to what has been discussed in Section 4). We note that in principle one could exchange the operators $\mathcal{L}_1$ and $\mathcal{L}_2$:

$$\mathcal{L}_1(\mathbf{u}) = \frac{q}{m}[0, 0, 0, E_r, E_\theta, E_z]^T, \tag{131}$$

and

$$\mathcal{L}_2(\mathbf{u}) = \left[v_r, \frac{v_\theta}{r}, v_z, \frac{v_\theta^2}{r} + \frac{q}{m} v_\theta B_z, -\frac{v_r v_\theta}{r} - \frac{q}{m} v_r B_z, 0\right]^T. \tag{132}$$

Since the half steps involve only the electric field and no change in position, they can be combined in a single full time step which is now exact. We note that these two leap-frog cyclotronic movers are the same from a computational point of view, differing only by the choice of the initial half step.

Table 4 shows the convergence study of the error measures (105)–(108) obtained with the leap-frog cyclotronic mover [according to operators (131) and (132)] for test particle 2. Comparing Tables 1 and 4, one can see that the errors associated with the radial coordinate [Eqs. (105) and (107)] have decreased by an order of magnitude, while the errors associated with the axial coordinate [Eqs. (106) and (108)] have decreased roughly by a factor of three. This is because, for test particle 2, the changes in r are influenced more by the magnetic field (i.e. the gyromotion) and therefore are now captured more accurately. On the other hand, the change in z is affected more by the electric field, which is algorithmically treated in the same way by the Boris and leap-frog cyclotronic movers. Table 4 also shows that overall the scheme is second order accurate in time. We also note that with our C implementation the leap-frog cyclotronic mover is $\sim 20\%$ faster than the classic Boris mover and about 50% faster than the standard cyclotronic mover with three steps.

Fig. 5(left) shows the trajectory in (r, z) for test particle 2 obtained with Method 1 and with the leap-frog cyclotronic mover with $\Delta t = 0.05$. In this simulation, the strength of the magnetic field has been increased to $B_z = 50$. Comparing with Fig. 2 (obtained with $B_z = 2$), one can see that the gyroradius (which is inversely proportional to the strength of the magnetic field) is greatly reduced and the particle radial position is localized near the radial injection position. Fig. 5(right) shows a zoom of the particle trajectory: while the particle gyromotion is not resolved very well due to the large Δt ($\omega \Delta t = 2.5$), the trajectory points are always very close to the reference solution. This is also confirmed by the error measures (105)–(108): $\mathrm{Err}_1 = 3.18 \cdot 10^{-4}$, $\mathrm{Err}_2 = 2.34 \cdot 10^{-3}$, $\mathrm{Err}_3 = 7.33 \cdot 10^{-4}$, and $\mathrm{Err}_4 = 3.59 \cdot 10^{-4}$.

7. Conclusions

In this paper, we have analyzed and compared different algorithms to study the dynamics of charged particles in a given electromagnetic field in cylindrical geometry. First, we have focused on the classic Boris mover. In the Boris algorithm,

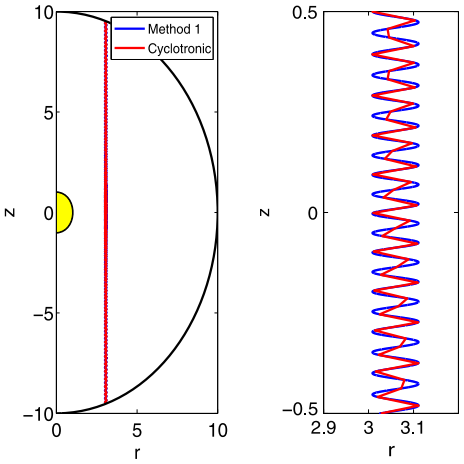

Fig. 5. Particle trajectory in (r, z) space obtained with Method 1 (blue line) and with the leap-frog cyclotronic mover (red line, $\Delta t = 0.05$) for test particle 2 with $B_z = 50$ (left). Zoom of the particle trajectory (right). The injection parameters are discussed in the caption of Table 2. (For interpretation of the references to color in this figure, the reader is referred to the web version of this article.)

positions and velocities of the particles are staggered in time and the inertial and electromagnetic forces are treated in an operator splitting fashion. The position and velocity update of the Boris algorithm is an exact update of the particle equation of motion under the action of inertial forces only. Furthermore, we have shown that the Boris algorithm can be connected to a second order Strang operator splitting method. For a finite magnetic field, the Boris and Strang mover are not exactly the same, but both are second order accurate methods. In general, the Boris mover should be favored over the Strang mover since it is about 20% faster without sacrificing much in terms of accuracy. Interestingly, unlike the case of Cartesian geometry, the Boris method is second order accurate only for a particular choice of the initial half step needed by the algorithm to get started, that is when $\mathbf{v}^{-1/2}$ is obtained by a first order backward formula that involves only the electromagnetic force. Any attempt to start with a more accurate $\mathbf{v}^{-1/2}$ decreases the order of accuracy of the method to first order. Through the connection with the Strang operator splitting method, this counter-intuitive behavior can be explained by fact that the error in the half step velocities in the Boris method is proportional to Δt or, in other words, these velocities are just auxiliary velocities used in the Strang mover to calculated the (second order accurate) velocities at integer steps. These theoretical considerations have been confirmed numerically, following the trajectories of test particles in a system consisting of a charged dust grain and an external, constant magnetic field.

For the case of a uniform and static magnetic field, we have rearranged the steps of the Strang splitting method to obtain the cylindrical analogue of the cyclotronic mover of Ref. [5]. This is done by combining the step involving acceleration due to the inertial forces with the acceleration due to the magnetic part of the Lorentz force. This algorithm can be made of leap-frog type by concatenating consecutive half steps, and remains second order accurate, symplectic and time reversible. The advantage of the cyclotronic mover is that it decouples the gyromotion from the rest of the dynamics and therefore relaxes the constraints on the time step that can arise in explicit electrostatic PIC simulations of strongly magnetized plasmas, where the gyromotion can be much faster than other frequencies of interest in the system [5].

We have only studied particle movers in cylindrical (r, θ, z) geometry. Alternatively, one could solve the equation of motion directly in Cartesian geometry. This has the advantage that one does not have to treat the inertial forces (and the associated singularity) and deals with simpler equations. On the other hand, for application in a cylindrical PIC code, one will have to transform the electromagnetic fields (from cylindrical to Cartesian geometry) and the particle position (from Cartesian to cylindrical, for the interpolation) at every time step. This increases the algorithmic complexity of the mover. We have implemented the Cartesian Boris mover in C, including the transformations just described to mimic its application in a cylindrical PIC code, and found that it has the same accuracy but is $\sim 20\%$ slower than the cylindrical Boris mover. The latter should therefore be preferred.

Acknowledgements

The authors wish to thank John Finn for useful discussions on symplectic orbit integrators. This work was funded by the Laboratory Directed Research and Development program (LDRD), U.S. Department of Energy Office of Science, Office of Fusion Energy Sciences, under the auspices of the National Nuclear Security Administration of the U.S. Department of Energy by Los Alamos National Laboratory, operated by Los Alamos National Security LLC under contract DE-AC52-06NA25396.

References

[1] C.K. Birdsall, A.B. Langdon, Plasma Physics Via Computer Simulation, Taylor & Francis, 2004.
[2] R. Hockney, J. Eastwood, Computer Simulation Using Particles, Taylor & Francis, 1988.

[3] W. Daughton, V. Roytershteyn, H. Karimabadi, L. Yin, B.J. Albright, B. Bergen, K.J. Bowers, Role of electron physics in the development of turbulent magnetic reconnection in collisionless plasmas, Nature Physics 7 (7) (2011) 539–542.
[4] J.P. Boris, Relativistic plasma simulation–optimization of a hybrid code, in: Proceedings of the Fourth Conference on Numerical Simulation of Plasmas, Naval Research Laboratory, Washington, D.C., 1970, pp. 3–67.
[5] L. Patacchini, I. Hutchinson, Explicit time-reversible orbit integration in Particle In Cell codes with static homogeneous magnetic field, Journal of Computational Physics 228 (7) (2009) 2604–2615.
[6] W.H. Press, S.A. Teukolsky, W.T. Vetterling, B.P. Flannery, Numerical Recipes: The Art of Scientific Computing, 3rd edition, Cambridge University Press, 2007.
[7] R.I. McLachlan, M. Perlmutter, Energy drift in reversible time integration, Journal of Physics A: Mathematical and General 37 (45) (2006) L593–L597.
[8] J. Wallace, J. Brackbill, D. Forslund, Implicit moment electromagnetic plasma simulation in cylindrical coordinates, Journal of Computational Physics 63 (2) (1986) 434–457.
[9] N. Barboza, Heavy ion beam transport in an inertial confinement fusion reactor, Fusion Engineering and Design 32–33 (1996) 453–466.
[10] L. Cao, W. Pei, Z. Liu, T. Chang, B. Li, C. Zheng, PIC-MC code to model fast electron beam transport through dense matter, Plasma Science and Technology 8 (3) (2006) 269–274.
[11] R. Ringle, 3DCylPIC—a 3D particle-in-cell code in cylindrical coordinates for space charge simulations of ion trap and ion transport devices, International Journal of Mass Spectrometry 303 (1) (2011) 42–50.
[12] G. Lapenta, Democritus: An adaptive particle in cell (PIC) code for object–plasma interactions, Journal of Computational Physics 230 (12) (2011) 4679–4695.
[13] G. Strang, On the construction and comparison of difference schemes, SIAM Journal on Numerical Analysis 5 (3) (1968) 506–517.
[14] L. Patacchini, I.H. Hutchinson, G. Lapenta, Electron collection by a negatively charged sphere in a collisionless magnetoplasma, Physics of Plasmas 14 (2007) 062111.
[15] R. Marchand, PTetra, a tool to simulate low orbit satellite–plasma interaction, IEEE Transactions on Plasma Science 40 (2012) 217–229.
[16] G.L. Delzanno, E. Camporeale, J.D. Moulton, J.E. Borovsky, E.A. MacDonald, M.F. Thomsen, CPIC: a curvilinear Particle-In-Cell code for spacecraft–plasma interaction studies, submitted to IEEE Transaction on Plasma Science (2012).
[17] G.L. Delzanno, G. Lapenta, M. Rosenberg, Attractive potential around a thermionically emitting microparticle, Physical Review Letters 92 (2004) 035002.
[18] G.L. Delzanno, A. Bruno, G. Sorasio, G. Lapenta, Exact orbital motion theory of the shielding potential around an emitting, spherical body, Physics of Plasmas 12 (6) (2005) 62102-1–62102-18.